Induction of a Specific Strong Polyantigenic Cellular Immune Response after Short-Term Chemotherapy Controls Bacillary Reactivation in Murine and Guinea Pig Experimental Models of Tuberculosis[▽]

Evelyn Guirado,[1,2] Olga Gil,[1,2] Neus Cáceres,[1] Mahavir Singh,[3]
Cristina Vilaplana,[1,2] and Pere-Joan Cardona[1,2]*

Unitat de Tuberculosi Experimental, Department of Microbiology, Fundació Institut per a la Investigació en Ciències de la Salut Germans Trias i Pujol, Universitat Autònoma de Barcelona, Crta del can Ruti s/n, 08916 Badalona, Catalonia, Spain[1]; Ciber Enfermedades Respiratorias, Palma de Mallorca, Spain[2]; and Lionex Diagnostics and Therapeutics GMBH, Braunschweig, Germany[3]

RUTI is a therapeutic vaccine that is generated from detoxified and liposomed *Mycobacterium tuberculosis* cell fragments that has demonstrated its efficacy in the control of bacillus reactivation after short-term chemotherapy. The aim of this study was to characterize the cellular immune response generated after the therapeutic administration of RUTI and to corroborate the lack of toxicity of the vaccine. Mouse and guinea pig experimental models were infected with a low-dose *M. tuberculosis* aerosol. RUTI-treated animals showed the lowest bacillary load in both experimental models. RUTI also decreased the percentage of pulmonary granulomatous infiltration in the mouse and guinea pig models. This was not the case after *Mycobacterium bovis* BCG treatment. Cellular immunity was studied through the characterization of the intracellular gamma interferon (IFN-γ)-producing cells after the splenocytes' stimulation with *M. tuberculosis*-specific structural and growth-related antigens. Our data show that the difference between the therapeutic administration of BCG and RUTI resides mainly in the stronger activation of IFN-γ$^+$ CD4$^+$ cells and CD8$^+$ cells against tuberculin purified protein derivative, ESAT-6, and Ag85B that RUTI generates. Both vaccines also triggered a specific immune response against the *M. tuberculosis* structural antigens Ag16kDa and Ag38kDa and a marked mRNA expression of IFN-γ, tumor necrosis factor, interleukin-12, inducible nitric oxide synthase, and RANTES in the lung. The results show that RUTI's therapeutic effect is linked not only to the induction of a Th1 response but also to the stimulation of a quicker and stronger specific immunity against structural and growth-related antigens that reduces both the bacillary load and the pulmonary pathology.

Tuberculosis (TB) was one of the first infectious diseases for which an etiologic agent, the bacterium *Mycobacterium tuberculosis*, was identified, more than 100 years ago. In fact, it was one of the first pathogens to which a vaccine, the *Mycobacterium bovis* BCG vaccine, was developed (7, 23). In spite of this, *M. tuberculosis* still generates a latent tuberculosis infection (LTBI) in one-third of humans and kills 2 million people every year, more than any other infectious disease, including AIDS and malaria (43). This fact implies a fabulous reservoir of TB that renders the objective of controlling the disease in the short or middle term very difficult. These data clearly indicate that developing therapies against LTBI remains a priority and that new vaccines and drugs are needed to control it. In addition, it is crucial to better understand the nature of LTBI to enable the development of new antituberculous tools.

It has been proposed that the induction of intragranulomatous necrosis and the stressful extracellular environment (in which bacilli find a local environment with a low pH, a high number of catalytic enzymes, and a mixture of toxic radicals), as well as the specific immune response, are responsible for inducing nonreplicating bacilli (NRB), which are related to LTBI (12).

Classical observations have demonstrated that NRB are different from actively growing bacilli, because they are more able to resist stressful conditions (heat, low pH, and reactive oxygen intermediates) (25, 41), which may be why immunity against *M. tuberculosis* is triggered mainly against actively growing bacilli. Immunity against growing bacilli is focused on soluble antigens that are related to the multiplication of the bacilli, such as the ESAT-6/CFP-10 or antigen 85 (Ag85) complex (2). Little is known about the main antigens related to NRB, although they seem to be related to the induction of the DosR operon, as is the alpha crystallin (encoded by *acr*). Also known as the heat shock protein (encoded by *hspX*) of 16 kDa (Ag16kDa), it is one of the more expressed antigens (40).

The present gold standard therapy against LTBI is based on the administration of isoniazid (INH) for a 9-month period (14). The fact that INH is active only against growing bacilli led to the elaboration of the dynamic hypothesis of LTBI (12). That dynamic hypothesis is based on the idea that LTBI persists as a consequence of the constant endogenous reinfection

* Corresponding author. Mailing address: Unitat de Tuberculosi Experimental, Department of Microbiology, Fundació Institut per a la Investigació en Ciències de la Salut Germans Trias i Pujol, Crta del can Ruti, camí de les escoles s/n, 08916 Badalona, Catalonia, Spain. Phone: 34 93 497 86 86. Fax: 34 93 497 86 54. E-mail: pjcardona.igtp.germanstrias@gencat.cat.
▽ Published ahead of print on 4 June 2008.

by NRB, which are drained from the intragranulomatous necrosis areas by foamy macrophages (FM). By reaching the alveolar fluid, these NRB are able to form part of the aerosols induced to condition the inspired air (5). When INH is administered for a long period, the host has the opportunity to drain all of the NRB without having the risk of reinfection.

We previously observed that the cessation of chemotherapy in the TB murine model led to the reactivation of bacillary growth and also lowered the local immunological response (10). We hypothesized that the quick increase of the immunological response that was achieved with the immediate administration of the RUTI vaccine after a short period of chemotherapy inhibited the reactivation of any remaining bacilli (mainly NRB) (12). The antigenic composition of RUTI, made with fragmented *M. tuberculosis* cells grown under stressful conditions, might be wide enough to help boost or induce new specific T cells. These T cells recognize epitopes shown by new macrophages, which come to the remaining granulomas to phagocytize NRB; these various epitopes obtained from stressed bacilli provided by the RUTI vaccine otherwise would remain invisible to the usual immune response. In fact, this invisibility could be explained by the fact that they would be presented mainly by already-activated macrophages, including FM, that would suppress the specific T cells that rose against them (9). That is why a short-term chemotherapy that clears both FM and activated macrophages from the granuloma (9, 10) may allow the entrance of naïve macrophages that then will be able to present those antigens from NRB and to exert a bactericidal activity against them.

So far, RUTI already has demonstrated its efficacy in controlling *M. tuberculosis* infection in mouse and guinea pig experimental models after a short period of chemotherapy (13). The mechanism of action of RUTI has been partially studied, by the quantification of different immunoglobulin G isotypes against fragments of *M. tuberculosis* through Western blotting, and is characterized by the induction of a mixed Th1/Th2/Th3 strong polyantigenic response (8). It also has been related to the increase of tuberculin purified protein derivative (PPD)-specific gamma interferon-positive (IFN-γ^+), CD8$^+$ T cells in the lung, a fact not demonstrated by BCG in a therapeutic way (13). RUTI also plays a crucial role in controlling the reactivation of *M. tuberculosis* infection in SCID mice after receiving serum from mice treated with RUTI, thus demonstrating the protective role of the antibody-mediated immunity (18).

On the other hand, it has been postulated that therapeutic vaccination is toxic for the host already infected by *M. tuberculosis*, an effect known as the Koch phenomenon (24, 33, 37). The development of RUTI also is based on previous experiences of our group, in which we related the Koch phenomenon to a kind of local Schwartzmann reaction that was caused by endotoxin-like molecules rather than being caused by a specific immunity triggered against *M. tuberculosis* (11, 19). To avoid such reactions, *M. tuberculosis* fragments used in the RUTI vaccine are cleaned with Triton in order to remove those endotoxin-like molecules from the cell wall surface. The demonstration of a lack of toxicity is also a paramount issue in the development of vaccines. For this reason, we also have tested the efficacy of RUTI in the guinea pig model, which has a special susceptibility to the reinoculation of *M. tuberculosis* antigens (28).

The present study confirms that the inoculation of RUTI induces a polyantigenic cell-mediated immune response after short-term chemotherapy that is related to the reduction of both the bacillary load and pulmonary pathology.

(Parts of this study were presented at the Keystone Symposia—Tuberculosis: from Lab Research to Field Trials, Vancouver, British Columbia, Canada, 20 to 25 March 2007.)

MATERIALS AND METHODS

Animals. Specific-pathogen-free, 6-week-old, female C57BL/6 mice and female outbred Dunkin-Hartley guinea pigs (weighing 200 to 240 g at the beginning of the experiment) were provided by Harlan Iberica (Sant Feliu de Codines, Catalonia, Spain).

The animals were shipped in appropriate conditions with corresponding certificates of health and origin. All animals were kept under standard controlled conditions in an animal P3 level high-security facility with sterile food and water ad libitum.

Animal health. Mice were checked every day by following a protocol that paid attention to weight loss, apparent good health (bristled hair and wounded skin), and behavior (signs of aggressiveness or isolation). Guinea pigs were weighed once a week and checked every day for pain and distress by using a modified Karnofsky scale (22). Mice were euthanized with a halothane overdose and guinea pigs with ketamine (100 mg/kg of body weight) plus diazepam (5 mg/kg) in order to avoid any suffering. Sentinel animals were used to check specific-pathogen-free conditions in the facility. Tests for 25 known mouse pathogens all were negative.

All experimental proceedings were approved and supervised by the Animal Care Committee of Germans Trias i Pujol University Hospital in agreement with the European Union laws for the protection of experimental animals.

Bacteria and infection. (i) Bacteria. *M. tuberculosis* strain H37Rv Pasteur was grown in Proskauer Beck medium containing 0.01% Tween 80 to mid-log phase and stored at −70°C in 2-ml aliquots.

(ii) *M. tuberculosis* aerosol infection. For infection, animals were placed in the exposure chamber of an airborne infection apparatus (Glas-col Inc., Terre Haute, IN). The nebulization provided an approximate uptake of 20 to 50 bacilli to mouse lungs and 10 bacilli to guinea pig lungs (9, 13).

(iii) CFU. The number of viable bacteria in target organs was determined by plating serial dilutions of whole-organ homogenates on nutrient Middlebrook 7H11 agar (Biomedics, s.l., Madrid, Spain) and counting the bacterial colonies after 21 days of incubation at 37°C. Special care was taken to avoid hiliar lymph nodes when removing the left lungs of mice to prevent an artificial increase in the number of CFU. Data were expressed as the log$_{10}$ of the mean number of bacteria recovered per organ.

(iv) RUTI. RUTI vials were kindly provided by Archivel Farma, s.l. (Badalona, Catalonia, Spain), manufactured under strict good manufacturing practice standards, as published elsewhere (8). Briefly, *M. tuberculosis* H37Rv cells were cultured for 3 weeks on Middlebrook 7H11 agar at 37°C, and colonies were carefully removed and mechanically disrupted using silica-zirconia beads in phosphate-buffered saline (PBS) with 4% Triton X-114. After centrifugation at 3,000 × g to remove undisrupted cells, the pellet was centrifuged at 27,000 × g, the lipidic supernatant was removed, and the final product was washed and pasteurized at 65°C for 50 min and then lyophilized. This product is called FCMtb (for fragmented cells of *M. tuberculosis*). Finally, liposomes were prepared after mixing the cell extracts at high speed with phosphatidylcholine and sodium cholate (20:1.4). The peptide composition of RUTI was determined using sodium dodecyl sulfate-polyacrylamide gel electrophoresis and Western blot analysis, as previously described (8).

In this study, different batches of RUTI were used: batch B04 (with 277 μg of FCMtb) in the mouse experiment and batches A03 (with 245 μg of FCMtb) and A04 (with 262 μg of FCMtb) in the guinea pig ones.

(v) Antigens. PPD and BCG antigens were obtained from the Statens Serum Institute (SSI; Copenhagen, Denmark). The rest of the antigens, ESAT-6, Ag85B, Ag16kDa (also known as HspX or acr), and Ag38kDa, were kindly provided by Lionex Diagnostics and Therapeutics GmbH (Braunschweig, Germany) (Table 1).

Treatments and immunizations. (i) Chemotherapy. Studies were carried out with aerosol-infected mice and guinea pigs (Fig. 1). Mice were orally treated with INH plus rifapentin (RPN) (25 and 10 mg/kg, respectively) once a week from weeks 6 to 14 postinfection. Guinea pigs were orally treated using INH plus

TABLE 1. Characteristics of the antigens used

Antigen (locus tag)	Recombinant or natural	Manufacturer
PPD	Natural	SSI
ESAT-6 (Rv3875)	Recombinant	Lionex
Ag16kDa (Rv2031c)	Recombinant	Lionex
Ag85B (Rv1886c)	Recombinant	Lionex
Ag38kDa (Rv0934)	Recombinant	Lionex
BCG	Natural	SSI

TABLE 2. Pathology scoring in the lungs of guinea pigs[a]

Value (points)	Type of lesion
0	No visible lesions
1	1 Lesion of <2 mm in diam
2	<5 Lesions of <2 mm in diam
3	>6 Lesions of <2 mm in diam or a single distinct gross lesion of >5 mm in diam
4	>1 Lesion of >5 mm in diam
5	1 Coalescent lesion

[a] One point is added for each coalescent lesion (10 maximum); 0.1 point is added for each lesion of <2 mm in diameter.

rifampin (RIF) (25 and 10 mg/kg, respectively) in a 5% sucrose solution, 5 days a week from weeks 4 to 8.

(ii) **Immunotherapy.** In the mouse model, three groups of animals were defined. The control and the RUTI group received PBS or RUTI, respectively, at fixed time points. The third group, the BCG group, received a single dose of BCG (2×10^6 CFU) at week 14 and PBS at week 17. The experiments were repeated twice for mice. For guinea pigs, the first experiment was stopped at week 16 for CFU determination. In this case, only two experimental groups were included (control and RUTI treated). The BCG treatment group was included in the experiment devoted to the study of the pathology, which ended at week 24 (Fig. 1).

(iii) **Measurement of DTH.** For the delayed hypersensitivity response (DTH) evaluation, each mouse received an injection of PPD (batch RT-49; 5 μg) into the hind footpad. Swelling at the hind footpad was measured by an engineer's micrometer before and 24 h after the infection.

(iv) **Histology and morphometry of mice.** Procedures for the histology and morphometry of mice have been described previously (18). Briefly, two right-lung lobes from each mouse were fixed in buffered formalin and subsequently embedded in paraffin. Every sample was stained with hematoxylin-eosin, thrichromic of Masson, and Ziehl Neelsen.

For histometry, 5-μm-thick sections from each specimen were stained with hematoxylin-eosin and photographed at ×6 magnification using a Stereoscopic Zoom SMZ800 microscope (Nikon, Tokyo, Japan) and a Coolpix 990 digital camera (Nikon). Sections of eight lung lobes were studied in each case. A sequence of appropriate software programs was used, Scion Image (Scion Corporation, Frederick, MD) and then Photoshop 5.0 (Adobe Systems Incorporated, San José, CA), to determine the area of each single lesion and the total tissue area on photomicrographs. Sections were blindly evaluated in order to get a more objective measurement.

(v) **Pathology score in lung of guinea pigs.** All lung lobes, left apical, left cardiac, left diaphragmatic, right apical, right cardiac, and right diaphragmatic, were examined individually, and the pathology scoring was quantified using standards adapted from Vordermeier et al. (39), as detailed in Table 2.

Ex vivo analysis of antigen-specific T cells. (i) IFN-γ intracellular staining and flow cytometry. Cell suspensions obtained from splenocytes of individual mice, at different weeks postinfection, were cultured (5×10^5 cells/well) overnight with the antigens in a 96-well round-bottom plate at 37°C and 5% CO_2.

Stimuli were used at a final concentration of 10 μg/ml for PPD and 5 μg/ml for ESAT-6, Ag85B, Ag38kDa, and Ag16kDa. Cells stimulated with no-azide/low-endotoxin-concentration anti-mouse CD3 (CD3 ε chain; clone 145-2C11) plus no-azide/low-endotoxin-concentration anti-mouse CD28 (clone 37.51) served as positive controls. Cells stimulated with medium alone served as negative controls. The following antibodies used for immunophenotyping were purchased from BD Biosciences: fluorescein isothiocyanate anti-mouse CD4 (L3T4; clone RM4-5), phycoerythrin-Cy5 anti-mouse CD8a (Ly-2; clone 53-6.7), peridinin-chlorophyll protein anti-mouse CD45 (leukocyte common antigen Ly-5; clone 30-F11), allophycocyanin anti-mouse IFN-γ (clone XMG1.2), and an allophyco-cyanin anti-mouse immunoglobulin G1 isotype control.

Intracellular staining was assayed with a flow cytometry Cytofix/Cytoperm fixation/permeabilization solution kit and BD GolgiStop (BD Biosciences, San Diego, CA) according to the manufacturer's recommendations. In brief, surface and intracytoplasmic antigen staining were performed sequentially. The inhibition of IFN-γ secretion was done with GolgiStop (monensin) for an additional 4 h, and cells were washed twice with staining buffer (1% fetal calf serum in PBS). Cells were stained first for surface markers (20 min at 4°C in the dark), washed with staining buffer, and permeabilized with Cytofix/Cytoperm (50 μl). Finally, cells were incubated with anti-IFN-γ antibody (30 min at 4°C in the dark). Unbound antibody was removed by washing the cells; cells were resuspended in permeabilization/wash buffer and transferred to fluorescence-activated cell sorter tubes.

A total of 250,000 cells from the lymphocyte gate for each sample were acquired for analysis. Data were collected using a flow cytometer (FACSCalibur; BD Biosciences, San Diego, CA) and analyzed using CellQuest Pro software (BD Biosciences, San Diego, CA). Lymphocytes were identified by their char-
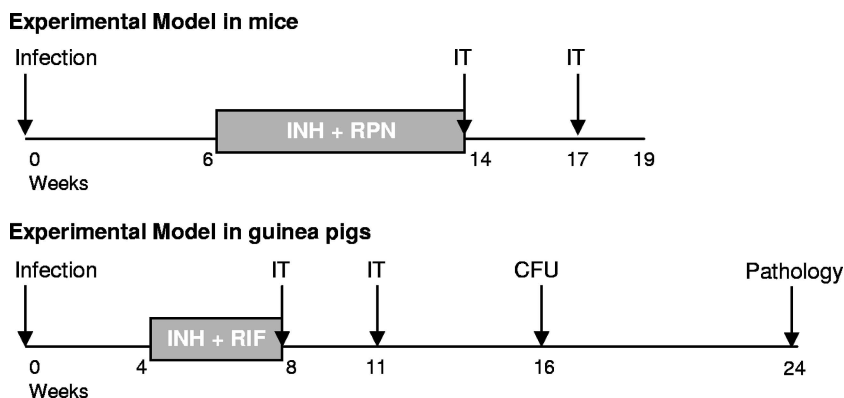

FIG. 1. Experiment designs. In both experimental animal models, animals were infected with a low-dose H37Rv aerosol. Treatment with immunotherapy (IT) with RUTI or BCG was administered after a short-term chemotherapy with INH plus RPN in mice or INH plus RIF in guinea pigs. The experiments were repeated twice in mice. The first guinea pig experiment was stopped at week 16 for the determination of the number of CFU. In this case, only two experimental groups were included (control and RUTI treated). A BCG treatment group was included in the experiment that was devoted to the pathology study, which ended at week 24.
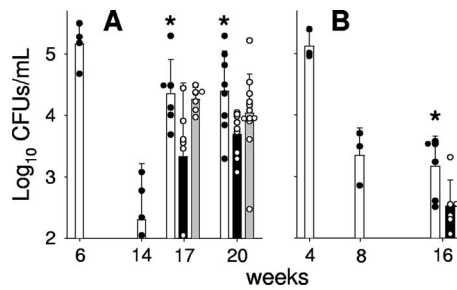
FIG. 2. Bacillary load in lungs of aerosol-infected mice and guinea pigs. (A) After infection, mice were treated with INH/RPN from weeks 6 to 14 (in white) and with two subcutaneous inoculations of RUTI at weeks 14 and 17 (in black) or BCG at week 14 (in gray). (B) After infection, guinea pigs were treated with INH/RIF from weeks 4 to 8 (in white) and with two subcutaneous inoculations of RUTI at weeks 8 and 11 (in black). The results are given as mean values with SD obtained from 4 (weeks 6 and 14) to 12 mice or three (weeks 4 and 8) to six guinea pigs for each time point. An asterisk indicates significant differences ($P < 0.05$ by t test). The color of the asterisk corresponds to the group with lower values to which the comparison was significant (i.e., black asterisks refer to the RUTI group).
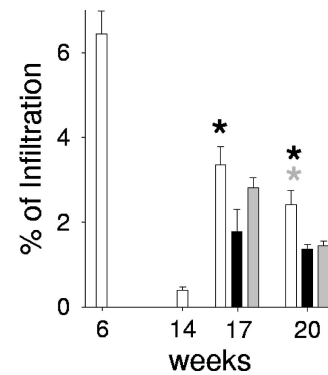

FIG. 3. Quantification of granulomatous infiltration in aerosol-infected mice's lung. After infection, mice were treated with INH/RPN from weeks 6 to 14 (in white) and with two subcutaneous inoculations of RUTI at weeks 14 and 17 (in black) or BCG at week 14 (in gray). Also shown are the percentages of pulmonary infiltration, which were obtained by dividing the area of granulomatous infiltration by the total area of the lobes, multiplied by 100. Values represent the means and SD. An asterisk indicates significant differences ($P < 0.05$ by t test). The color of the asterisk corresponds to the group with lower values to which the comparison was significant. Black and gray asterisks refer to RUTI and BCG groups, respectively.

acteristic size (by forward light scatter) and granularity (by side light scatter) and by lymphocyte surface phenotype.

(ii) ELISPOT assay. Activated antigen-specific IFN-γ secreting T cells were detected using the BD murine IFN-γ enzyme-linked immunospot (ELISPOT) assay kit (BD Bioscience, San Diego, CA) according to the manufacturer's recommendations. Briefly, cell suspensions obtained from the spleens of individual mice, at different weeks postinfection, were added to wells at an initial concentration of 2.5×10^5 cells/well.

Cells were stimulated with PPD (10 μg/ml), BCG (10^6 CFU), ESAT-6, Ag85B, Ag16kDa, and Ag38kDa (all of them at a final concentration of 5 μg/ml). Cells stimulated with phorbol myristate acetate (5 ng/ml; Sigma) plus ionomycin (500 ng/ml; Sigma) served as positive controls, whereas nonstimulated cells served as negative controls. The plate was incubated overnight at 37°C and 5% CO_2.

The next day, the plate was incubated with detection antibody (a biotinylated anti-mouse IFN-γ antibody) for 2 h at room temperature. Unbound detection antibody was removed by washing the cells, and the enzyme conjugate (streptavidin-horseradish peroxidase) was added. After 1 h of incubation at room temperature, unbound enzyme conjugate was removed by washing the plate, and the plate was stained with a 3-amino-9-ethylcarbazole substrate solution for 20 min. The plate was washed and allowed to air dry overnight, and spot-forming units (SFU) were counted using an ELISPOT reader.

(iii) mRNA quantification. Protocols for mRNA quantification have been described elsewhere (9). In short, the middle right lobe of the lungs was removed and frozen with RNA Later (Ambion, Austin, TX) at −20°C for the extraction of total mRNA. RNA extraction was performed using TRIzol (Gibco BRL, Grand Island, NY) in combination with FastPrep products (Qbiogene Inc., Illkirch, France). Lysing matrix B tubes were filled with an adequate volume of TRIzol, and samples were homogenized in a FastPrep FP120 cell fragmenter for two cycles of 45 and 20 s at maximum speed, with chilling on ice between cycles. Subsequent steps of RNA extraction were performed by following the manufacturer's recommendations.

The total RNA concentration was determined by spectrophotometry with a nanodrop (Nanodrop Technologies Inc., Wilmington, DE), and a denaturing agarose gel was used to check RNA stability. Total RNA was subjected to a DNase treatment with a DNA-free kit (Ambion, Austin, TX).

Five micrograms of RNA then was reverse transcribed using a Transcriptor reverse transcriptase kit (Roche Biochemicals, Idaho Falls, ID) according to the manufacturer's recommendations, using oligo(dT) (Gibco BRL) to obtain cDNA. The quantitative analysis of IFN-γ, tumor necrosis factor alpha (TNF-α), inducible nitric oxide synthase (iNOS), RANTES, interleukin-4 (IL-4), IL-10, and IL-12p40 was performed using a LightCycler system (Roche Biochemicals, Idaho Falls, ID). Real-time PCR was carried out in glass capillaries to a final volume of 10 μl in the presence of 1 μl of 10× reaction buffer (*Taq* polymerase, deoxynucleoside triphosphates, and Sybr green), 1 μl of cDNA (or water as a negative control), $MgCl_2$ to a final concentration of 0.8 mM, and primers to a final concentration of 0.5 μM.

Following PCR, a single peak was present in the melting curve analysis, corresponding to a single species of the appropriate estimated size in agarose gel electrophoresis. The expression of hypoxanthine guanine phosphoribosyl transferase (HPRT) mRNA expression was analyzed for every target sample to normalize for efficiency in cDNA synthesis and RNA loading. A ratio based on the HPRT mRNA expression was obtained for each sample.

Statistical analysis. SigmaStat 3.5 (Systat Software Inc., San José, CA) was used to compare values. Data were expressed as the means ± standard deviations (SD). Statistical significance was determined using a paired two-tailed Student t test or one-way analysis of variance test. Differences were significant at $P < 0.05$.

RESULTS

Immunotherapy with RUTI after short-term chemotherapy reduces the number of bacilli in the lungs. Figure 2 shows the effect of RUTI administration on the bacterial load in both mouse and guinea pig experimental models. All mice showed reactivation after chemotherapy, and although no bactericidal effect was observed, the RUTI-treated group showed the lowest bacterial load. In the guinea pig model, no reactivation was seen in the control group, but a bactericidal effect was shown after RUTI vaccination (Fig. 2B). Figure 2A also shows that the BCG inoculation did not change the bacterial load in the mouse model.

RUTI and BCG treatment controls pulmonary infiltration in the lungs and does not cause any toxic effect. Since the granulomatous infiltration response plays a critical role in controlling mycobacterial dissemination, we examined the percentage of pulmonary granulomatous infiltration, defined as the ratio obtained after dividing the infiltrated area by the total area of the lung section, and then multiplied it by 100. The results showed that 3 weeks after the chemotherapy cessation, the percentage of pulmonary granulomatous infiltration was significantly decreased in the RUTI group compared to those of the control and BCG groups (Fig. 3); interestingly, 6 weeks later (at week 21) this decrease also was noticed in the BCG group. The quality of the lesions did not differ among the experimental groups, and

neither intragranulomatous nor pyogranulomatous necrosis was detected in any case.

In the experimental model with guinea pigs, all of the pulmonary lobes were examined individually. A pathology-scoring method adapted from studies on cattle (39) was applied to quantify the severity of disease. A slight reduction in the number of lung lobes infected and a reduced lung pathology score were noticed in both the RUTI- and BCG-vaccinated animals, as the pathology scores were reduced to 54.3% and 68.04%, respectively, of the one induced in the control group.

Inoculation of RUTI increases the DTH response in mice. The DTH response against PPD was threefold increased in RUTI-vaccinated animals (0.18 ± 0.07 mm) compared to the response of the BCG-vaccinated ones (0.05 ± 0.08 mm) at week 17 postinfection. Swelling in the control group animals was undetectable.

RUTI increased the percentage of antigen-specific T cells in the murine experimental model. The IFN-γ intracellular staining results showed that in both the control and the BCG-treated groups, the percentage of $CD4^+$ and $CD8^+$ IFN-γ^+ T cells tended to be lower than that in RUTI-vaccinated mice, especially after the second inoculation of RUTI (18 and 20 weeks postinfection). These differences were significant when the cells were stimulated with PPD, ESAT-6, or Ag85B, although increases of $CD8^+$ cells were seen in the control group against Ag85B (week 18) and in the BCG-vaccinated group against PPD and Ag85B (week 15). In contrast, differences between mice vaccinated with RUTI or BCG usually were not seen after stimulation with the 16- or 38-kDa proteins, as in both cases the results tended to be higher than those for the control group. Again, a high increase in 38-kDa $CD8^+$ cells also was induced in the BCG group at week 18 (Fig. 4).

ELISPOT results indicated that the number of SFU per 250,000 cells was higher after the RUTI inoculation than for other groups. The most remarkable fact was that 1 week after the first and second inoculations of RUTI (week 15 and week 18), there was a high increase in IFN-γ-secreting cells against ESAT-6, Ag85B, and PPD compared to the response of the other two groups. Only at week 20 was there an equivalent value for ESAT-6-stimulated cells in the control group, probably as a consequence of the high bacillary reactivation (Fig. 5). In all cases, reactivity was obtained mainly against PPD, ESAT-6, and Ag85B, while the response against Ag16kDa and Ag38kDa was lower.

mRNA expression of IFN-γ, TNF-α, IL-4, IL-10, IL-12p40, iNOS, and RANTES. To assess whether the increased protection against *M. tuberculosis* infection seen in RUTI-treated mice was associated with a change in the cytokine production in the lung, the mRNA expression of IFN-γ, TNF-α, IL-4, IL-10, IL-12p40, iNOS, and RANTES from these tissues was analyzed in the various models.

The local cytokine expression in lung samples revealed an increase in the mRNA expression of IFN-γ, TNF-α, IL-12, iNOS, and RANTES at week 17 postinfection in the groups treated with BCG or RUTI compared to that of the group treated only with chemotherapy. Interestingly, this response tended to be higher in the BCG group. At week 18, there was a decrease in the expression in both immunotherapy-treated groups (except for TNF-α), which was less apparent in the group treated with RUTI. In contrast, the control group
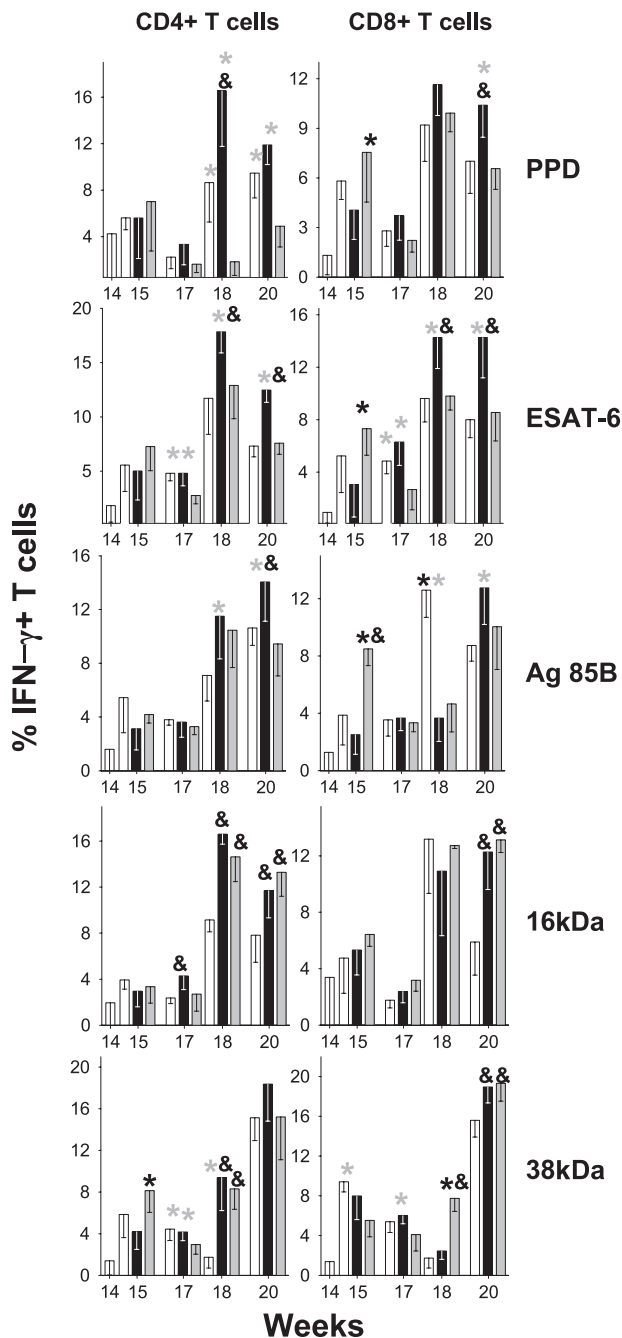

FIG. 4. Evolution of $CD4^+$ and $CD8^+$ IFN-γ^+-specific cells from spleen in aerosol-infected mice. After infection, mice were treated with INH/RPN from weeks 6 to 14 (in white) and with two subcutaneous inoculations of RUTI at weeks 14 and 17 (in black) or BCG at week 14 (in gray). Data are expressed as the percentages of means and SD. An asterisk or ampersand indicates significant differences ($P < 0.05$ by t test). The color of the asterisk corresponds to the group with lower values to which the comparison was significant. Black and gray asterisks refer to RUTI and BCG groups, respectively; the ampersand refers to the control group.

showed a rise in all cytokines except for IFN-γ and iNOS. Finally, at week 20 cytokine levels were maintained in the immunotherapy groups, whereas in the control group there was a marked rise, probably as a consequence of the increased
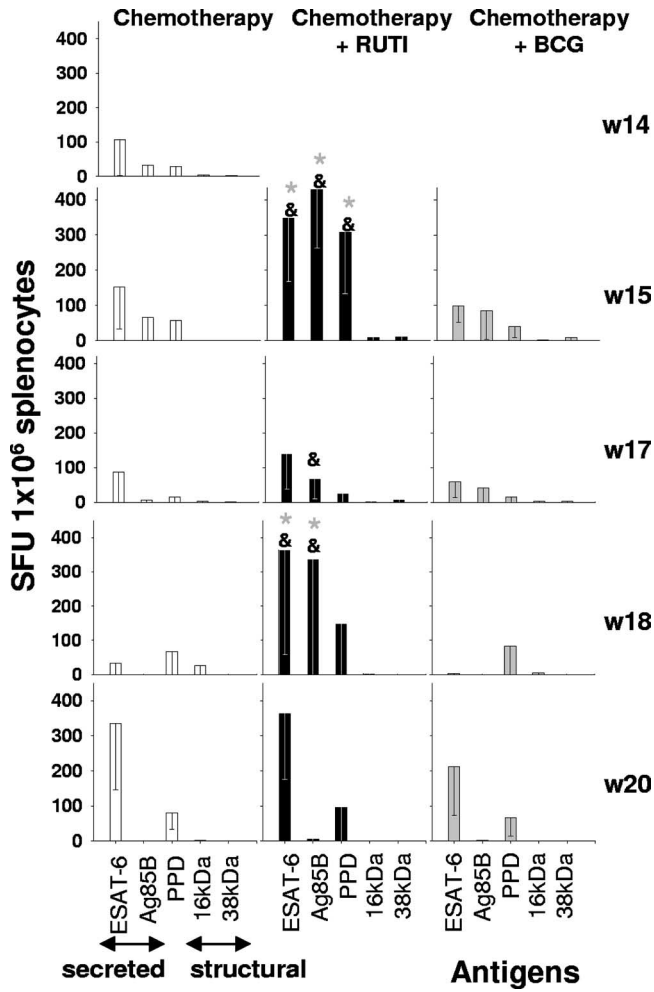
FIG. 5. Activated antigen-specific IFN-γ-secreting cells from the spleen of aerosol-infected mice. After infection, mice were treated with INH/RPN from weeks 6 to 14 (in white) and with two subcutaneous inoculations of RUTI at weeks 14 and 17 (w14 and w17, respectively; in black) or BCG at week 14 (in gray). Data represent the means and SD. An asterisk or ampersand indicates significant differences ($P < 0.05$ by t test). The color of the asterisk corresponds to the group with lower values to which the comparison was significant. Gray asterisks refer to the BCG group; the ampersand refers to the control group.

FIG. 6. Evolution of mRNA expression of IFN-γ, TNF-α, IL-12, iNOS, and RANTES in lungs at different time points. After infection, mice were treated with INH/RPN from weeks 6 to 14 (in white) plus two subcutaneous inoculations of RUTI at weeks 14 and 17 (in black) or BCG at week 14 (in gray). Data are expressed as the $\log_{10}$ of the ratio obtained after dividing every value by the expression of HPRT in each sample and multiplying it by a factor (ranging from 10^1 to 10^6). Data represent the means and SD. An asterisk or ampersand indicates significant differences ($P < 0.05$ by t test). The color of the asterisk corresponds to the group with lower values to which the comparison was significant. Black and gray asterisks refer to RUTI and BCG groups, respectively; the ampersand refers to the control group.

number of CFU. No expression of IL-10 and IL-4 was detected in any mouse group (Fig. 6). Interestingly, 1 week after RUTI inoculation (week 15), there was a significant decrease in TNF in this group compared to levels of TNF in the other ones, a fact that can be linked to a decreased intragranulomatous infiltration in the lungs and to a lower possibility of generating a local Schwartzmann reaction.

DISCUSSION

The use of therapeutic vaccines against TB has been a controversial issue since Robert Koch declared the usefulness of an *M. tuberculosis* culture extract (the tuberculin) as a therapeutic agent against initial stages of TB (6). Although tuberculin did not become the definitive cure of TB, it still became widely used as a therapeutic tool, together with other hygienic
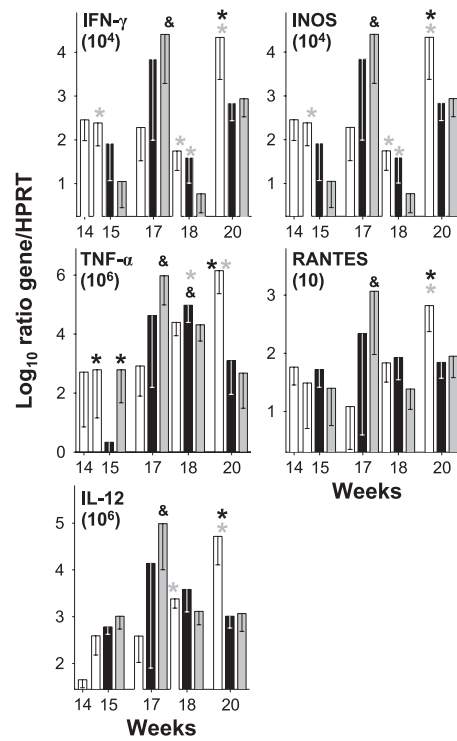
treatments, until the appearance of chemotherapy (29). Robert Koch himself, however, also demonstrated the usefulness of tuberculin as a diagnostic tool in a process linked to a toxic reaction, now known as the Koch reaction, and described that 4 to 6 weeks after the establishment of infection in guinea pigs, the intradermal challenge with whole organisms or culture filtrate resulted in local necrosis in the original tuberculous lesion (33).

More recently, the Stanford group developed another vaccine with heat-killed *Mycobacterium vaccae*. Initially, its therapeutic effect was attributed to the capacity of the antigens present in the *M. vaccae* cell wall to develop a Th1 immune response and to avoid a Th2 response. This idea came from the concept of *Listeria*-like and Koch-like responses (34). The former was related to a typical Th1 mechanism and induced nonnecrotic granulomas, while the latter was related to a Th2 mechanism and, thus, was responsible for the intragranulomatous necrosis generated by *M. tuberculosis* infection, which was considered to be negative. The Th2 response should be counterbalanced in order to control the infection better and to avoid the development of TB (21, 31). The comparison of IFN-γ/IL-4 ratios measured by different techniques after the

stimulation of T cells has generated controversial results (32); moreover, many theories have been postulated to explain the observed polarization of T-cell responses. Recent findings suggest that IL-4δ2 counterbalances IL-4 effects (4) or that T-regulatory cells counterbalance Th2 responses. Unfortunately, although several clinical trials have been run with *M. vaccae*, little or no effectiveness has been demonstrated in TB treatment (35).

The data presented here suggest that the most important mechanism of action of RUTI is linked not only to the induction of a Th1 immunological response but also to the induction of such a response specifically against *M. tuberculosis* structural and growth-related antigens. RUTI induces an increased number of specific $CD4^+$ and $CD8^+$ effector T cells and IFN-γ-secreting cells in the spleen, together with a restricted dissemination of bacilli in the lungs of infected mice. We have previously demonstrated that RUTI produces a Th1-Th2-Th3 equilibrated immune response instead of the pure Th1 response that should have more efficacy (20, 30). Recent data demonstrated a Th1-Th2 BCG response was as efficient as a Th1 response alone (17). On the other hand, it is interesting that RUTI did not induce an mRNA expression that would favor a local Schwartzmann reaction, i.e., increased levels of TNF (11). In fact, its expression 1 week after the first inoculation (week 15) was significantly the lowest one of the groups.

The benefits of RUTI are obtained after prior treatment with chemotherapy. By reducing the load of *M. tuberculosis*, this short period of chemotherapy allows a decrease in the immunological response and local inflammatory response in lungs, which normally is induced by growing bacilli (10). The chemotherapy also removes the accumulation of activated macrophages and FM from the granuloma, because of the reduction of the concentration of growing bacilli that led to a reduction of the inflammatory response. This fact has been demonstrated by a decrease in local TNF expression (10) and the histological findings (13). These cells are important inducers of local immunosuppression (36); thus, they probably play a key role in neutralizing any therapeutic vaccination. Reducing the bacillary load also may minimize the development of a local Koch reaction, as we have previously demonstrated (15).

Recent studies recommend against using postinfection vaccines with killed or live mycobacteria, as they could induce strong toxicity (24, 37). In the manufacturing procedure of RUTI, the vaccine is detoxified by removing endotoxin-like molecules to avoid the potential risk of developing a Schwartzmann reaction (8, 11). In both experiments with mice and guinea pigs, except for a transient local inflammatory response at the injection site, the inoculation of RUTI did not induce local or systemic toxicity.

It has been demonstrated that the control of the latent state of *M. tuberculosis* is dependent on the $CD8^+$ IFN-γ^+ cells (38), a finding that must be taken into consideration in the development of new vaccines against LTBI. RUTI increases $CD4^+$ IFN-γ^+ and $CD8^+$ IFN-γ^+ populations after stimulation with antigens related to growing and nongrowing bacilli. In previous studies (13), we demonstrated that while the therapeutic administration of RUTI or BCG enhanced 10-fold the size of the $CD4^+$ IFN-γ^+ PPD-specific population, only RUTI was able to enhance the $CD8^+$ IFN-γ^+ population in the lungs. A hypothesis for this finding is that its delivery through liposomes is crucial, as a substantial quantity of mycobacterial antigens could be presented by major histocompatibility complex class I, which may favor a CD8 response (1).

On the other hand, our study also reflects increases in the $CD8^+$ population in control and BCG groups at weeks 15 and 18, respectively. This fact could be due to the bacillary reactivation tested with both groups, as indicated elsewhere (1), but in the BCG group it also could be related to the presence of BCG bacilli in the spleen, which are able to induce strong CD8 responses (26).

The comparison of the immune responses of RUTI- and BCG-treated mice also highlights the higher response against ESAT-6, Ag85B, and PPD elicited by RUTI. This different trend may explain why BCG has no efficacy when given in a therapeutic way, a fact previously demonstrated by others (24). It is well known that ESAT-6 and Ag85B have a paramount role in the induction of a protective response (2); the majority of vaccines currently in development include either both antigens, one of them, or fusion proteins containing them (3). As infected hosts already have this immunity, this observation supports the theory that the protective effect of RUTI is linked to the boost of this previous immunity. This boosting would counterbalance the local immunodepression induced by the chemotherapy treatment, which would allow NRB to reactivate once stopped (10, 12).

Furthermore, recently it has been demonstrated that BCG needs to survive in vaccinated animals to generate specific immunity, so that if the vaccine is cleared by chemotherapy, the number of effector cells gradually decreases to the normal state and the protection wanes (27). The fact that BCG needs to grow to be effective (17) also may explain its lack of efficacy because, since the vaccinated host already has immunity against mycobacteria, it can curtail its multiplication. Interestingly, BCG inoculation does increase the pulmonary mRNA expression of Th1-related cytokines. This fact is not related to an increase in the bacillary control in this model.

On the other hand, due to previous data (8), a wide immune response triggered by RUTI against structural antigens like Ag16kDa or Ag38kDa (2) was expected, which would help the surveillance of NRB after short-term chemotherapy, by triggering or even boosting the proliferation of those specific T cells naturally induced by the destruction of the bacilli. This proliferation disappears over time (2), probably because of the pressure of the constant reactivation of the bacilli that is needed to maintain the LTBI, which will focus the immunity against the more dangerous bacillary form, the growing one (12). The fact that the response against structural antigens has been weakly demonstrated in the ELISPOT assay can be a consequence of the magnitude of the bacillary challenge. In this case, the immune response is directed mainly against the small bacillary population that is slowly drained to the lymph nodes, where they finally grow, as has been recently demonstrated (42). In humans, the ability to induce intragranulomatous necrosis from the very beginning, both in lungs and lymph nodes (16), generates a higher concentration of extracellular dead bacilli that can reach the spleen, so the chance to develop immunity against structural antigens can be higher.

Research on new vaccines against LTBI is difficult because of the lack of a validated method to correlate vaccine effectiveness in animal models and in humans. Consequently, the

limitations of the present work, which was carried out in small-animal models, must be highlighted. The results obtained for the validation of new immunotherapy treatments such as RUTI must be interpreted with caution. To mimic what really happens in humans, we used the chronic TB murine model, which was induced by low-dose aerosol, because of the similarities existing between this model and LTBI in humans in terms of the route of infection and the bacillary population in the chronic phase, which can be considered mainly nonreplicating (25, 41). We consider that further studies using experimental models with bigger animals (that are able to induce a human-like inflammatory response) are needed in order to study the nature of the antigenic response. We decided to run experiments with the guinea pig model in order to avoid the TB tolerance phenomenon observed in mice, which may underestimate new treatments against LTBI (13), but unfortunately, the techniques to explore the guinea pig immune response are limited. The guinea pig model develops a structured and defined granuloma with strong fibrosis and intragranulomatous necrosis. It is remarkable that the improved control of bacillary loads in the guinea pig model requires a bigger inflammatory response than can be observed in mice; in contrast, mice cannot develop such a high inflammatory response, because it would kill the host faster than the bacilli (13). Mice that trigger a weaker immune response, with no well-structured granulomas, with discrete fibrosis, without necrosis, and permitting the constant dissemination of bacilli throughout their lungs, are able to survive longer. Our hypothesis is that the bigger the host, the stronger the inflammatory response against *M. tuberculosis*, because a big parenchyma can be destroyed in larger animals to stop bacillary growth. For this reason, we are carrying out more experiments in hosts with a volume more comparable to that of humans, like naturally infected goats or the mini-pig experimental model, in which the techniques to explore the immune response are more developed.

REFERENCES

1. **Altin, J. G., and C. R. Parish.** 2006. Liposomal vaccines—targeting the delivery of antigen. Methods **40:**39–52.
2. **Andersen, P.** 1997. Host responses and antigens involved in protective immunity to Mycobacterium tuberculosis. Scand. J. Immunol. **45:**115–131.
3. **Andersen, P.** 2007. Tuberculosis vaccines—an update. Nat. Rev. Microbiol. **5:**484–487.
4. **Atamas, S. P., J. Choi, V. V. Y. Yurovsky, and B. White.** 1996. An alternative splice variant of human IL-4, IL4 delta 2, inhibits IL-4-stimulated T cell proliferation. J. Immunol. **156:**435–441.
5. **Bui, T. D., D. Dabdub, and S. C. George.** 1998. Modeling bronchial circulation with application to soluble gas exchange: description and sensitivity analysis. J. Appl. Physiol. **84:**2070–2088.
6. **Burke, D. S.** 1993. Of postulates and peccadilloes: Robert Koch and vaccine (tuberculin) therapy for tuberculosis. Vaccine **11:**795–804.
7. **Calmette, A., and H. Plotz.** 1929. Protective inoculation against tuberculosis with BCG. Am. Rev. Tuberc. **19:**567–572.
8. **Cardona, P. J., I. Amat, S. Gordillo, V. Arcos, E. Guirado, J. Díaz, C. Vilaplana, G. Tapia, and V. Ausina.** 2005. Immunotherapy with fragmented Mycobacterium tuberculosis cells increases the effectiveness of chemotherapy against a chronical infection in a murine model of tuberculosis. Vaccine **23:**1393–1398.
9. **Cardona, P. J., S. Gordillo, J. Díaz, G. Tapia, I. Amat, A. Pallares, C. Vilaplana, A. Ariza, and V. Ausina.** 2003. Widespread bronchogenic dissemination makes DBA/2 mice more susceptible than C57BL/6 mice to experimental aerosol infection with *Mycobacterium tuberculosis*. Infect. Immun. **71:**5845–5854.
10. **Cardona, P. J., E. Julian, X. Valles, S. Gordillo, M. Muñoz, M. Luquin, and V. Ausina.** 2002. Production of antibodies against glycolipids from the Mycobacterium tuberculosis cell wall in aerosol murine models of tuberculosis. Scand. J. Immunol. **55:**639–645.
11. **Cardona, P. J., R. Llatjos, S. Gordillo, J. Diaz, B. Vinado, A. Ariza, and V. Ausina.** 2001. Towards a 'human-like' model of tuberculosis: intranasal inoculation of LPS induces intragranulomatous lung necrosis in mice infected aerogenically with Mycobacterium tuberculosis. Scand. J. Immunol. **53:**65–71.
12. **Cardona, P. J.** 2006. New insights on the nature of latent tuberculosis infection and its treatment. Inflam. Allerg. Drug Targ. **6:**27–39.
13. **Cardona, P. J.** 2006. RUTI: a new chance to shorten the treatment of latent tuberculosis infection. Tuberculosis (Edinburgh) **86:**273–289.
14. **Comstock, G. W.** 1999. How much isoniazid is needed for prevention of tuberculosis among immunocompetent adults? Int. J. Tuberc. Lung Dis. **3:**847–850.
15. **Gil, O., E. Guirado, S. Gordillo, J. Diaz, G. Tapia, C. Vilaplana, A. Ariza, V. Ausina, and P. J. Cardona.** 2006. Intragranulomatous necrosis in lungs of mice infected by aerosol with Mycobacterium tuberculosis is related to bacterial load rather than to any one cytokine or T cell type. Microb. Infect. **8:**628–636.
16. **Grange, J. M.** 1998. Immunophysiology and immunopathology of tuberculosis, p. 113–127. *In* P. D. O. Davies (ed.), Clinical tuberculosis, vol. 8. Chapman & Hall, London, United Kingdom.
17. **Gruppo, V., and I. M. Orme.** 2002. Dose of BCG does not influence the efficient generation of protective immunity in mice challenged with Mycobacterium tuberculosis. Tuberculosis (Edinburgh) **82:**267–273.
18. **Guirado, E., I. Amat, O. Gil, J. Díaz, V. Arcos, N. Cáceres, V. Ausina, and P. J. Cardona.** 2006. Passive serum-therapy with polyclonal antibodies against Mycobacterium tuberculosis protects against post-chemotherapy relapse of tuberculosis infection in SCID mice. Microb. Infect. **8:**1252–1259.
19. **Guirado, E., S. Gordillo, O. Gil, J. Diaz, G. Tapia, C. Vilaplana, V. Ausina, and P. J. Cardona.** 2006. Intragranulomatous necrosis in pulmonary granulomas is not related to resistance against Mycobacterium tuberculosis infection in experimental murine models induced by aerosol. Int. J. Exp. Pathol. **87:**139–149.
20. **Hernandez-Pando, R., L. Pavon, K. Arriaga, H. Orozco, V. Madrid-Marina, and G. Rook.** 1997. Pathogenesis of tuberculosis in mice exposed to low and high doses of an environmental mycobacterial saprophyte before infection. Infect. Immun. **65:**3317–3327.
21. **Hernandez-Pando, R., and G. A. Rook.** 1994. The role of TNF-alpha in T-cell-mediated inflammation depends on the Th1/Th2 cytokine balance. Immunology **82:**591–595.
22. **Karnofsky, D. A., W. H. Abelmann, L. F. Craver, and J. H. Burchenal.** 1948. The use of nitrogen mustards in the palliative treatment of cancer. Cancer **1:**634–656.
23. **Koch, R.** 1882. Classics in infectious diseases. The etiology of tuberculosis: Robert Koch, Berlin, Germany. Rev. Infect. Dis. **4:**1270–1274.
24. **Moreira, A. L., L. Tsenova, M. H. Aman, L. G. Bekker, S. Freeman, B. Mangaliso, U. Schroder, J. Jagirdar, W. N. Rom, M. G. Tovey, V. H. Freedman, and G. Kaplan.** 2002. Mycobacterial antigens exacerbate disease manifestations in *Mycobacterium tuberculosis*-infected mice. Infect. Immun. **70:**2100–2107.
25. **Muñoz-Elías, E. J., J. Timm, T. Botha, W. T. Chan, J. E. Gomez, and J. D. McKinney.** 2005. Replication dynamics of *Mycobacterium tuberculosis* in chronically infected mice. Infect. Immun. **73:**546–551.
26. **Murray, R. A., N. Mansoor, R. Harbacheuski, J. Soler, V. Davids, A. Soares, A. Hawkridge, G. D. Hussey, G. Maecker, G. Kaplan, and W. A. Hanekom.** 2006. Bacillus Calmette Guerin vaccination of human newborns induces a specific, functional CD8+ T cell response. J. Immunol. **177:**5647–5651.
27. **Olsen, A. W., L. Brandt, E. M. Agger, L. A. H. Van Pinxteren, and P. Andersen.** 2004. The influence of remaining live BCG organisms in vacci-

nated mice on the maintenance of immunity to tuberculosis. Scand. J. Immunol. **60:**273–277.

28. **Orme, I. M.** 2005. The use of animal models to guide rational vaccine design. Microb. Infect. **7:**905–910.

29. **Pottenger, F. M.** 1934. Tuberculosis in the child and the adult. The C.V. Mosby Company, St. Louis, MO.

30. **Power, C. A., G. Wei, and P. A. Bretscher.** 1998. Mycobacterial dose defines the Th1/Th2 nature of the immune response independently of whether immunization is administered by the intravenous, subcutaneous, or intradermal route. Infect. Immun. **66:**5743–5750.

31. **Rook, G. A., and R. al Attiyah.** 1991. Cytokines and the Koch phenomenon. Tubercle **72:**13–20.

32. **Rook, G. A., R. Hernandez-Pando, K. Dheda, and G. T. Seah.** 2004. IL-4 in tuberculosis: implications for vaccine design. Trends Immunol. **25:**483–488.

33. **Rook, G. A., and R. Hernandez-Pando.** 1996. The pathogenesis of tuberculosis. Annu. Rev. Microbiol. **50:**259–284.

34. **Stanford, J. L., M. J. Shield, and G. A. Rook.** 1981. How environmental bacteria may predetermine the protective efficacy of BCG. Tubercle **62:** 55–62.

35. **Stanford, J., C. Stanford, and J. Grange.** 2004. Immunotherapy with Mycobacterium vaccae in the treatment of tuberculosis. Front. Biosci. **9:**1701–1719.

36. **Stumbles, P. A., A. S. McWilliam, and P. G. Holt.** 1999. Dendritic cells and mucosal macrophages, p. 397–412. *In* P. L. Ogra, J. Mestecky, M. E. Lamm, W. Strober, J. Bienenstock, and J. R. McGhee (ed.), Mucosal immunology. Academic Press, San Diego, CA.

37. **Turner, J., E. R. Rhoades, M. Keen, J. T. Belisle, A. A. Frank, and I. M. Orme.** 2000. Effective preexposure tuberculosis vaccines fail to protect when they are given in an immunotherapeutic mode. Infect. Immun. **68:**1706–1709.

38. **Van Pinxteren, L. A. H., P. Cassidy, B. H. C. Smedegaard, E. M. Agger, and P. Andersen.** 2000. Control of latent Mycobacterium tuberculosis is dependent on CD8 T cells. Eur. J. Immunol. **30:**3689–3698.

39. **Vordermeier, H. M., M. A. Chambers, P. J. Cockle, A. O. Whelan, J. Simmons, and R. G. Hewinson.** 2002. Correlation of ESAT-6-specific gamma interferon production with pathology in cattle following *Mycobacterium bovis* BCG vaccination against experimental bovine tuberculosis. Infect. Immun. **70:**3026–3032.

40. **Voskuil, M. I., K. C. Visconti, and G. K. Schoolnik.** 2004. Mycobacterium tuberculosis gene expression during adaptation to stationary phase and low-oxygen dormancy. Tuberculosis (Edinburgh) **84:**218–227.

41. **Wallace, J. G.** 1961. The heat resistance of tubercle bacilli in the lungs of infected mice. Am. Rev. Respir. Dis. **83:**866–871.

42. **Wolf, A. J., L. Desvignes, B. Linas, N. Banaiee, T. Tamura, K. Takatsu, and J. D. Ernst.** 2008. Initiation of the adaptive immune response to Mycobacterium tuberculosis depends on antigen production in the local lymph node, not the lungs. J. Exp. Med. **205:**105–115.

43. **World Health Organization.** 2007. Global tuberculosis control—surveillance, planning, financing. WHO report 2007, Global tuberculosis control report. WHO/HTM/TB/2007.376. WHO, Geneva, Switzerland.